Resonance Raman Studies of Dinuclear Zirconium Complexes with a Bridging Dinitrogen Ligand. Possible N_2-Coordination Models for Nitrogenase

Jonathan D. Cohen,[1] Murugesapillai Mylvaganam,[2] Michael D. Fryzuk,*[,2] and Thomas M. Loehr*[,1]

Contribution from the Department of Chemistry, Biochemistry, and Molecular Biology, Oregon Graduate Institute of Science & Technology, Portland, Oregon 97291-1000, and the Department of Chemistry, University of British Columbia, Vancouver, British Columbia V6T 1Z1, Canada

Received April 13, 1994®

Abstract: Resonance Raman spectroscopy was used to investigate the vibrational properties of the bridging dinitrogen ligand in two different dinuclear zirconium complexes known to contain unusually long N–N bonds. $\{[(Pr^i_2PCH_2SiMe_2)_2N]Zr(\eta^5\text{-}C_5H_5)\}_2(\mu\text{-}\eta^1\text{:}\eta^1\text{-}N_2)$ (**1**) has an "end-on" bridging dinitrogen ligand and $\{[(Pr^i_2PCH_2SiMe_2)_2N]ZrCl\}_2(\mu\text{-}\eta^2\text{:}\eta^2\text{-}N_2)$ (**2**) has a "side-on" bridging dinitrogen ligand. The ν(N–N) stretching frequency for the $\mu\text{-}\eta^1\text{:}\eta^1\text{-}N_2$ complex is observed at 1211 cm^{-1} in the solid state and confirmed by an ~40-cm^{-1} isotope shift in the $^{15}N_2$-substituted isotopomer. A similar frequency and isotope shift are observed for **1** in toluene, indicating that the $\mu\text{-}\eta^1\text{:}\eta^1\text{-}N_2$ structure is preserved in solution. Vibrational assignments for the $\mu\text{-}\eta^2\text{:}\eta^2\text{-}N_2$ complex **2** are complicated by the presence of many isotope-sensitive peaks in the solid state. Nevertheless, we propose that the intense peak at ~731 cm^{-1} corresponds to one of the totally symmetric A_g modes of the Zr_2N_2 moiety that is predominantly ν(N–N) in character based on its ~22-cm^{-1} isotope shift and its strong polarization in THF solution. The majority of the remaining peaks in the resonance Raman spectrum of **2** can be assigned as overtone and combination bands of fundamental modes at 258, 317, and 393 cm^{-1} and the ν(N–N) mode at 731 cm^{-1} (709 cm^{-1} in the ^{15}N isotopomer). Comparison of solid and solution state data for **2** suggests that the structure of the side-on-bonded N_2 ligand is largely maintained in THF solution. Finally, the vibrational spectroscopic properties of **2** as the dibromo and the mixed bromochloro complex are reported. These complexes all maintain the strong ν(N–N) mode at 709 cm^{-1} (^{15}N isotopomers) but exhibit changes in the fundamental modes at ~300 cm^{-1} and, hence, also for the resulting overtone and combination bands. This work has shown that resonance Raman spectra reveal very marked differences and, hence, can be used to distinguish the two modes of bonding in side-on versus end-on coordinated N_2 complexes of dinuclear transition metals.

Introduction

Nitrogen fixation is the process by which N_2 is reduced to NH_3. Industrially, the reduction of N_2 to NH_3 is accomplished at ~150 atm and ~550 °C in the presence of H_2 using an iron-based catalyst in the well-known Haber–Bosch process. Biological nitrogen fixation occurs at ambient temperature and pressure when catalyzed by nitrogenase, a multiprotein complex found in nitrogen-fixing microorganisms.[3,4] The crystal structures of the MoFe proteins of the nitrogenases of *Azotobacter vinelandii* and *Clostridium pasteurianum* were recently reported.[5,6] These proteins contain a unique cofactor containing iron and molybdenum that is believed to be the site of N_2 reduction.[7] Unfortunately, the crystal structures of these proteins do not provide information regarding either the location or the geometry of substrate binding. Nonetheless, several molecular orbital simulations of N_2 binding as simplified variants of the FeMo cofactor have been investigated (*vide infra*).[8] The synthesis of iron–molybdenum clusters has been pursued vigorously in several laboratories in attempts to prepare functional models of the nitrogenase chemistry.[9–11] However, other transition-metal complexes of N_2 may also serve as model compounds to provide useful insights into N_2 bonding and activation through metal complexation.

In 1965, Allen and Senoff reported the synthesis of $[Ru(NH_3)_5N_2]^{2+}$, the first compound known to have a dinitrogen ligand terminally bound to a transition metal.[12] Since then, the catalog of complexes containing terminal and/or bridging N_2 ligands has grown immensely.[13–19] However, most of these complexes show little extension of the N–N bond from its gas-phase equilibrium value of 1.0975 Å.[20] Nevertheless, there are a few metal–dinitrogen complexes with N–N bond lengths significantly greater than ~1.1 Å.[21–28] Although lengthening of

® Abstract published in *Advance ACS Abstracts*, September 15, 1994.

(1) Oregon Graduate Institute of Science & Technology.

(2) University of British Columbia.

(3) Burris, R. H. *J. Biol. Chem.* **1991**, *266*, 9339–9342.

(4) (a) Dilworth, M. J.; Glenn, A. R., Eds. *Biology and Biochemistry of Nitrogen Fixation*; Elsevier: New York, NY, 1991. (b) Orme-Johnson, W. H. *Annu. Rev. Biophys. Biophys. Chem.* **1985**, *14*, 419–549.

(5) (a) Kim, J.; Rees, D. C. *Science* **1992**, *257*, 1677–1681. (b) Chan, M. K.; Kim, J.; Rees, D. C. *Science* **1993**, *260*, 792–794.

(6) (a) Kim, J.; Woo, D.; Rees, D. C. *Biochemistry* **1993**, *32*, 7104–7115. (b) Bolin, J. T.; Ronco, A. E.; Morgan, T. V.; Mortensen, L. E.; Xuong, N.-H. *Proc. Natl. Acad. Sci. U.S.A.* **1993**, *90*, 1078–1082.

(7) Orme-Johnson, W. H. *Science* **1992**, *257*, 1639–1640.

(8) Deng, H.; Hoffmann, R. *Angew. Chem., Int. Ed. Engl.* **1993**, *32*, 1062–1065.

(9) Coucouvanis, D. *Acc. Chem. Res.* **1991**, *24*, 1–8.

(10) Bose, K. S.; Chmielewski, S. A.; Eldredge, P. A.; Sinn, E.; Averill, B. A. *J. Am. Chem. Soc.* **1989**, *111*, 8953–8954.

(11) Holm, R. H.; Simhon, E. D. In *Molybdenum Enzymes*; Spiro, T. G., Ed.; Wiley-Interscience: New York, 1985; Chapter 1.

(12) Allen, A. D.; Senoff, C. V. *Chem. Commun.* **1965**, 621–622.

(13) (a) Sanner, R. D.; Duggan, M.; McKenzie, T. C.; Marsh, R. E.; Bercaw, J. E. *J. Am. Chem. Soc.* **1976**, *98*, 8358–8365. (b) Sanner, R. D.; Manriquez, J. M.; Marsh, R. E.; Bercaw, J. E. *J. Am. Chem. Soc.* **1976**, *98*, 8351–8357.

(14) Dilworth, J. R.; Richards, R. L. In *Comprehensive Organometallic Chemistry*; Wilkinson, G., Stone, F. G. A., Abel, E. W., Eds.; Pergamon Press: Oxford, 1982; Vol. 8, p 1073.

(15) Henderson, R. A.; Leigh, G. J.; Pickett, C. J. *Adv. Inorg. Chem. Radiochem.* **1983**, *27*, 197.

(16) Pelikán, P.; Boca, R. *Coord. Chem. Rev.* **1984**, *55*, 55–112.

(17) Evans, W. J.; Ulibarri, T. A.; Ziller, J. W. *J. Am. Chem. Soc.* **1988**, *110*, 6877–6879. This paper reports the first example of a $\mu\text{-}\eta^2\text{:}\eta^2\text{-}N_2$ structure in a dinuclear metal (samarium) complex. The N–N bond length was reported as 1.088 (12) Å, a value similar to that of N_2(g).

(18) (a) Leigh, G. J. *Sci. Prog. (Oxford)* **1989**, *291*, 389–412. (b) Leigh, G. J. *Acc. Chem. Res.* **1992**, *25*, 177–181.

(19) Henderson, R. A. *Transition Met. Chem.* **1990**, *15*, 330.

(20) Wilkinson, P. G.; Houk, N. B. *J. Chem. Phys.* **1956**, *24*, 528–534.

0002-7863/94/1516-9529$04.50/0

N–N 1.301(3) Å

$Zr–N_2$ 1.920(3) Å

Zr–N–N 170°

Zr–N' 2.306(3) Å

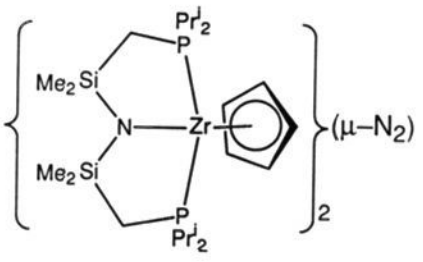

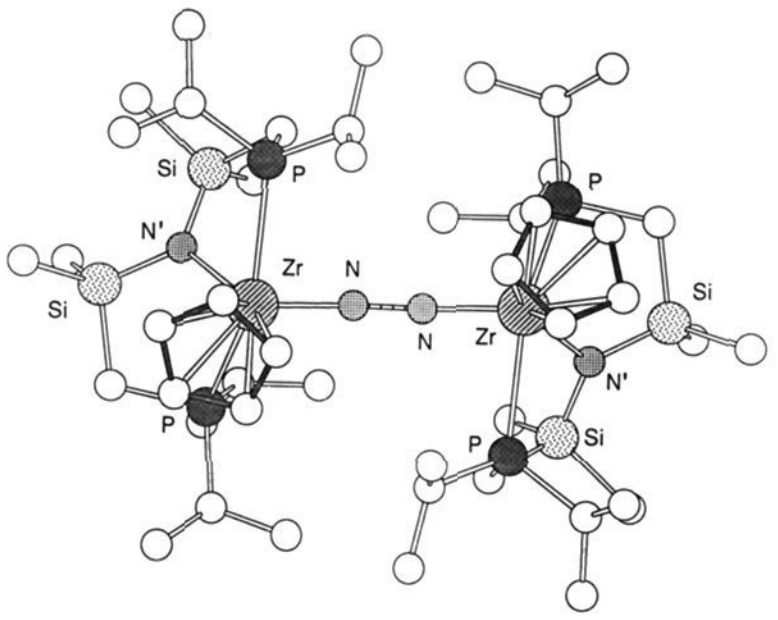

Figure 1. Molecular structure of complex **1** shown as a ball-and-stick model and several important $(\mu\text{-}\eta^1\text{:}\eta^1\text{-}N_2)Zr_2N'$ bonding parameters; adapted from ref 21.

N–N' 1.548(7) Å

Zr–N 2.024(4) Å

Zr–N1 2.175(3) Å

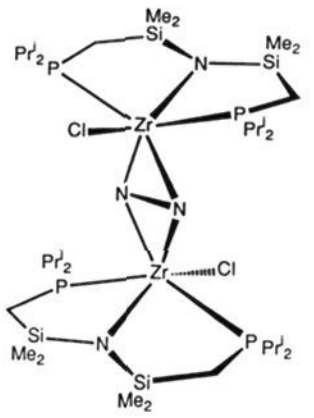

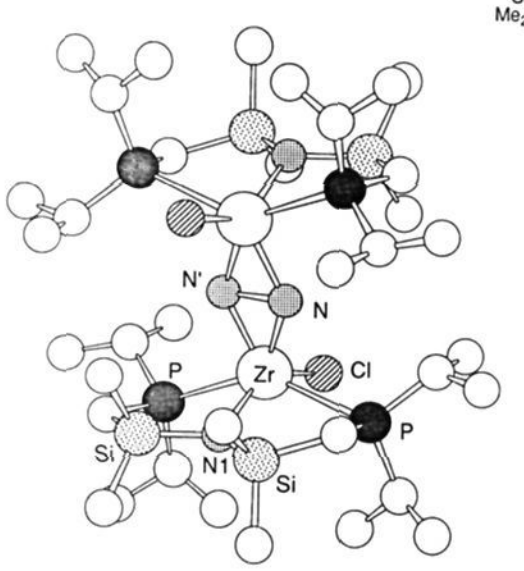

Figure 2. Molecular structure of complex **2** shown as a ball-and-stick model and several important $(\mu\text{-}\eta^1\text{:}\eta^1\text{-}N_2)Zr_2N'$ bonding parameters; adapted from ref 21.

the N_2 bond upon metal complexation does not, by itself, denote a particular compound's ability to fix nitrogen,[18b] one must logically conclude that elongation (accompanied by protonation) and eventual N–N bond dissociation are necessary for the reduction of 1 mol of N_2 to 2 mol of NH_3 in the biological reaction sequence.

Recently, two dinuclear zirconium–dinitrogen complexes with unusually long N–N bonds have been synthesized (Figures 1 and 2).[21] Complex **1**, $\{[(Pr^i_2PCH_2SiMe_2)_2N]Zr(\eta^5\text{-}C_5H_5)\}_2(\mu\text{-}\eta^1\text{:}\eta^1\text{-}N_2)$, has an N_2 ligand bridging the two Zr atoms with a nearly linear "end-on" geometry (Figure 1). Its N–N bond length of 1.301 Å determined from X-ray crystallography represents a very significant increase from that of the $N_2(g)$ equilibrium value.[21] Complex **2**, $\{[(Pr^i_2PCH_2SiMe_2)_2N]ZrCl\}_2(\mu\text{-}\eta^2\text{:}\eta^2\text{-}N_2)$, contains a rare example of an N_2 ligand bridging both metal atoms with "side-on" geometry and exhibits an N–N bond length of 1.548 Å in the crystal structure[21,29] (Figure 2). In fact, complex **2** has the longest reported N–N bond length for any metal–dinitrogen complex.[29] Deng and Hoffmann propose that this side-on geometry is one of the preferred coordination models of N_2 binding to the FeMo cofactor of nitrogenase based on the low calculated N–N overlap population, which facilitates bond dissociation, and the increased net negative charge on each of the nitrogen atoms necessary for protonation.[8]

For the two dinuclear Zr complexes **1** and **2**, semiempirical MO calculations have shown that the preference for end-on versus side-on binding of the dinitrogen ligand can be accounted for by suitable choices of the ancillary ligands.[21] However, attempts to extend the range of complexes that contain the rare side-on binding mode have been hampered by the fact that distinguishing between side-on and end-on modes of ligation is non-trivial. Infrared spectroscopy as well as solid- and solution-state ^{15}N-NMR spectroscopy have been decidedly ambiguous. Up to the present, only single-crystal X-ray crystallography has been unequivocal. In this paper, we report a resonance Raman (RR) study of these compounds to characterize the vibrational frequencies of end-on and side-on dinitrogen ligands in transition-metal complexes. In addition, we are interested in establishing the structural identity of these complexes in solution and determining if there is any structural isomerism of the dinitrogen ligand. Owing to the high local symmetry of the dinitrogen stretching mode, Raman and/or resonance Raman (RR) spectroscopy are the only analytical methods available to directly observe the N–N stretching frequency, and this technique has been previously used in the study of bridging N_2 complexes.[25,30] For the end-on complex **1**, we have identified ν(N–N) in the RR spectrum at 1211 cm^{-1} on the basis of its single isotope-sensitive frequency. In contrast, RR spectra of the side-on complex **2** show many isotope-sensitive bands; however, the predominant ν(N–N) is observed at 731 cm^{-1}. The remaining bands in the spectra of **2** are assigned to a few fundamental modes and to many overtone and combination bands of the Zr_2N_2 moiety. Moreover, in complex **2**, the position and intensity of the RR spectral features are sensitive to the nature of the ancillary ligands as well as to whether the sample is in the solid phase or in solution.

Experimental Section

Preparation of Compounds. Crystals and solutions of $\{[(Pr^i_2PCH_2SiMe_2)_2N]Zr(\eta^5\text{-}C_5H_5)\}_2(\mu\text{-}\eta^1\text{:}\eta^1\text{-}N_2)$ (**1**, reddish-brown, $\lambda_{max} \sim 490$ nm) and $\{[(Pr^i_2PCH_2SiMe_2)_2N]ZrCl\}_2(\mu\text{-}\eta^2\text{:}\eta^2\text{-}N_2)$ (**2**, deep blue, $\lambda_{max} \sim 580$

(21) Fryzuk, M. D.; Haddad, T. S.; Mylvaganam, M.; McConville, D. H.; Rettig, S. J. *J. Am. Chem. Soc.* **1993**, *115*, 2782–2792.
(22) Manriquez, J. M.; Sanner, R. D.; Marsh, R. E.; Bercaw, J. E. *J. Am. Chem. Soc.* **1976**, *98*, 3042–3044.
(23) Schrock, R. R.; Fellmann, J. D. *J. Am. Chem. Soc.* **1978**, *100*, 3359–3370.
(24) Messerle, L. W.; Jennische, P.; Schrock, R. R.; Stucky, G. D. *J. Am. Chem. Soc.* **1980**, *102*, 6744–6752.
(25) Campbell, J. R.; Clark, R. J. H.; Stead, M. J. *J. Chem. Soc., Dalton Trans.* **1983**, 2005–2010.
(26) Edema, J. J.; Meetsma, A.; Gambarotta, S. *J. Am. Chem. Soc.* **1989**, *111*, 6878–6880.
(27) (a) O'Regan, M. B.; Liu, A. H.; Finch, W. C.; Schrock, R. R.; Davis, M. W. *J. Am. Chem. Soc.* **1990**, *112*, 4331. (b) Schrock, R. R.; Kolodziej, R. M.; Liu, A. H.; Davis, M. W.; Vale, M. G. *J. Am. Chem. Soc.* **1990**, *112*, 4338–4345.
(28) Duchateau, R.; Gambarotta, S.; Beydoun, N.; Benison, C. *J. Am. Chem. Soc.* **1991**, *113*, 8986–8988.
(29) Fryzuk, M. D.; Haddad, T. S.; Rettig, S. J. *J. Am. Chem. Soc.* **1990**, *112*, 8185–8186.
(30) Kachapina, L. M.; Borshch, V. N.; Kichigina, G. A.; Makhaev, V. D.; Borisov, A. P. *Nouv. J. Chim.* **1982**, *6*, 253–258.

nm) were prepared by methods described elsewhere.[21] Isotopic substitution with $^{15}N_2$ was carried out by degassing the starting materials and introducing $^{15}N_2$ into the reaction mixture. Typical sample concentrations were between 100 and 300 mg/L. All samples were anaerobically sealed under nitrogen in 1.5–1.8 × 90 mm Kimax glass capillary tubes and stored at room temperature until studied.[31]

Synthesis of $[(Pr^i_2PCH_2SiMe_2)_2N]ZrBr_3$. To a suspension of $ZrBr_4$ (2.03 g, 4.94 mmol) in toluene (50 mL) was added a solution of $[(Pr^i_2PCH_2SiMe_2)_2N]Li$ (1.00 g, 2.50 mmol) in toluene (10 mL) at room temperature (RT). The reaction mixture was stirred for 16 h, and then the LiCl salt was removed by filtering through Celite. The filtrate was concentrated to 15 mL and hexanes were added until the solution turned turbid; cooling at −30 °C yielded a colorless crystalline product (1.12 g, 73%). ^{1}H NMR (δ, 200.123 MHz, C_6D_6): 0.41 (s, 12H, $Si(CH_3)_2$); 1.11 (m, 28H, $P[CH(CH_3)_2]_2$, $SiCH_2P$); 2.07 (sept of triplets, 4H, $P[CH(CH_3)_2]_2$, $^2J_{H-P}$ = 2.7 Hz, $^3J_{H-H}$ = 7.2 Hz). $^{31}P\{^1H\}$ NMR (δ 81.015 MHz, C_6D_6): 16.52 (s). $^{13}C\{^1H\}$ NMR (δ, 50.323 MHz, C_6D_6): 4.50 (s, $Si(CH_3)_2$); 11.93 (s, $SiCH_2P$); 18.85 (s, $P[CH(CH_3)_2]_2$); 19.12 (s, $P[CH(CH_3)_2]_2$); 25.14 (t, $P[CH(CH_3)_2]_2$, $^2J_{C-P}$ = 6.8 Hz). Anal. Calcd for $C_{18}H_{44}Br_3NP_2Si_2Zr$: C, 29.88; H, 6.13; N, 1.94. Found: C, 30.00; H, 6.30; N, 1.99.

Synthesis of $\{[(Pr^i_2PCH_2SiMe_2)_2N]ZrBr\}_2(\mu$-$\eta^2$:$\eta^2$-$N_2)$. A solution of $ZrBr_3[N(SiMe_2CH_2PPr^i_2)_2]$ (0.628 g, 0.943 mmol) in toluene (80 mL) was transferred into a thick-walled reaction flask (300 mL), equipped with a 10-mm Teflon needle valve, and containing 0.35% Na/Hg (24 g, 3.59 mmol). The flask was then cooled to −196 °C, filled with N_2, sealed, and allowed to warm slowly to RT with stirring. The colorless solution slowly takes on the deep blue color of the product. The reaction mixture was stirred for 7 days and then filtered through a layer of Celite. The amalgam-containing residue was extracted with several 80-mL portions (~1 L) of toluene until the extracts showed no blue color. Upon removal of the toluene under vacuum, the product separates out as crystalline material (0.23 g, 42%). ^{1}H NMR (δ, 300 MHz, C_7D_8): 0.30 (s, 12H, $Si(CH_3)_2$); 0.34 (s, 12H, $Si(CH_3)_2$); 1.02 (m, 8H, $SiCH_2P$); 1.44 (d of d, 12H, $P[CH(CH_3)_2]_2$, $^3J_{H-H}$ = 7.3 Hz, $^2J_{H-P}$ = 13.7 Hz); 1.24 (m, 36H, $P[CH(CH_3)_2]_2$); 2.18 (d of sept, 4H, $P[CH(CH_3)_2]_2$, $^3J_{H-H}$ = 7.5 Hz, $^2J_{H-P}$ = 4.2 Hz); 2.42 (d of sept, 4H, $P[CH(CH_3)_2]_2$, $^3J_{H-H}$ = 7.6 Hz, $^2J_{H-P}$ = 3.9 Hz). $^{31}P\{^1H\}$ NMR (δ, 121.4 MHz, C_7D_8): 9.96 (s). Anal. Calcd for $C_{18}H_{44}BrN_2P_2Si_2Zr$: C, 37.42; H, 7.68; N, 4.85. Found: C, 37.84; H, 7.84; N, 3.89. The lower nitrogen content found is probably due to the formation of nitrides during combustion.

Synthesis of $\{[(Pr^i_2PCH_2SiMe_2)_2N]ZrBr\}_2(\mu$-$\eta^2$:$\eta^2$-$^{15}N_2)$. The $^{15}N_2$ analogue was prepared by a procedure similar to the synthesis of the unlabeled compound by introducing $^{15}N_2$ gas into the flask containing the degassed reaction mixture at RT. Workup was carried out under unlabeled N_2. $^{15}N\{^1H\}$ NMR (δ, 30.406 MHz, THF/C_6D_6): 345.75 (s). MS: Calcd for M^+: 1158. Found (EI) m/z: 1158, 1113, 1025, 941, 895, 350, 262.

Synthesis of $\{[(Pr^i_2PCH_2SiMe_2)_2N]Zr\}_2ClBr(\mu$-$\eta^2$:$\eta^2$-$N_2)$. A solution containing a mixture of $ZrBr_3[N(SiMe_2CH_2PPr^i_2)_2]$ (0.160 g, 0.221 mmol) and $ZrCl_3[N(SiMe_2CH_2PPr^i_2)_2]$ (0.131 g, 0.222 mmol) was treated with 0.34% Na/Hg (12.2 g, 1.79 mmol) as described in the synthesis of $\{[(Pr^i_2PCH_2SiMe_2)_2N]ZrBr\}_2(\mu$-$\eta^2$:$\eta^2$-$N_2)$. $^1H\{^{31}P\}$ NMR (δ, 500 MHz, C_7D_8): 0.28 (s, $Si(CH_3)_2$); 0.29 (s, $Si(CH_3)_2$); 0.31 (s, $Si(CH_3)_2$); 0.32 (s, $Si(CH_3)_2$); 0.33 (s, $Si(CH_3)_2$); 0.34 (s, $Si(CH_3)_2$); 0.65 (m, $SiCH_2P$); 1.00 (m, $SiCH_2P$); 1.28 (m, $P[CH(CH_3)_2]_2$); 1.41 (m, $P[CH(CH_3)_2]_2$); 2.40 (m, $P[CH(CH_3)_2]_2$). $^{31}P\{^1H\}$ NMR (δ, 121.4 MHz, C_7D_8): 10.30 (s); 10.06 (s); 9.96 (s); 9.89 (s). MS: Calcd for M^+: 1111. Found (EI) m/z: 1111, 1067, 1023, 979, 262.

Synthesis of $\{[(Pr^i_2PCH_2SiMe_2)_2N]Zr\}_2ClBr(\mu$-$\eta^2$:$\eta^2$-$^{15}N_2)$. The $^{15}N_2$ analogue was prepared by a procedure similar to the synthesis of the unlabeled compound by introducing $^{15}N_2$ gas into the flask containing the degassed reaction mixture. Workup was carried out under unlabeled N_2. $^{15}N\{^1H\}$ NMR (δ, 30.406 MHz, C_4H_8O/C_6D_6): 352.50 (s, ~1N); 349.26 (s, ~2N); 345.75 (s, ~1N). MS: Calcd for M^+: 1113. Found (EI) m/z: 1113, 1069, 1025, 981, 895, 849, 350, 262.

Resonance Raman Spectroscopy.[32] Spectra were recorded at ~90 K by placing the capillaries containing the microcrystalline or the solution samples in a copper cold finger within a Dewar filled with liquid N_2. Raman spectra were obtained on a modified Jarrell-Ash Model 25-300 Raman spectrophotometer equipped with an RCA C31034 photomultiplier tube and controlled by an Intel 310 computer. Excitation radiation was supplied by Spectra Physics Ar^+ and Kr^+ lasers operating at 514.5 and 647.1 nm, respectively, and by a Coherent CR-599 dye (rhodamine 6G) laser tuned to 580 nm and pumped by a Coherent INNOVA 90-6 Ar^+ laser. Plasma emissions from the lasers were removed with an Applied Photophysics prism filter monochromator. Scattered radiation was collected in a backscattering geometry. Multiple scans were collected and calibrated against toluene, CCl_4, and/or THF. The reported frequency positions of all strong, sharp peaks are estimated to be accurate to ±2 cm^{-1}. Spectra for polarization studies of solution samples were collected in a 90°-scattering geometry at ~278 K on a DILOR Z-24 Raman spectrophotometer interfaced to an IBM PC/AT computer. Typical slit-width settings were between 5 and 10 cm^{-1}. All spectral data were analyzed and processed with GRAMS/386 or LabCalc (Galactic Industries, Salem, NH) or with Origin (MicroCal Software, Northampton, MA).

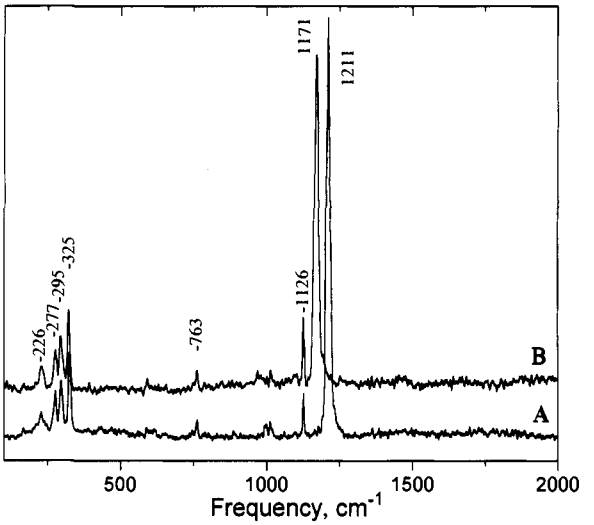

Figure 3. Resonance Raman spectra of complex **1** in the solid state at ~90 K: (A) μ-η^1:η^1-N_2, (B) μ-η^1:η^1-$^{15}N_2$ isotopomer. Each trace is a sum of 5 consecutive scans each recorded at 2 cm^{-1}/s using 40 mW of 514.5-nm laser excitation.

Results and Discussion

Vibrational Spectra of $Zr_2(\mu$-η^1:η^1-$N_2)$ Complexes. The RR spectra of complex **1** in the solid state and its $^{15}N_2$-enriched isotopomer are shown in Figure 3. For these experiments, only the nitrogen atoms of the bridging ligand are isotopically labeled. Clearly, the most prominent feature in Figure 3A is the strong peak at 1211 cm^{-1}. In addition, weaker peaks are apparent at 1126, 1012, 997, 763, 325, 295, 277, and 226 cm^{-1}. The 1211-cm^{-1} peak shifts to 1171 cm^{-1} in the μ-η^1:η^1-$^{15}N_2$-isotopomer (Figure 3B) and is the *only* feature to exhibit a significant isotope shift. The magnitude of this isotope shift is nearly equal to that predicted for a simple diatomic oscillator (calcd, 41 cm^{-1}; obsd, 40 cm^{-1}) and, thus, indicates that the observed mode is essentially a pure ν(N–N) stretching mode. Frequencies and the proposed assignment of ν(N–N) for complex **1** are given in Table 1.

The difference between the diatomic stretching frequency of N_2(g) reported[33] at 2331 cm^{-1} and the same vibration observed at 1211 cm^{-1} in complex **1** implies a significant elongation of the dinitrogen bond with a concomitant decrease in the N–N bond order from 3 in N_2(g) to a value between 1 and 2 in complex **1**. In Figure 4, the N–N frequencies for a number of dinitrogen-containing compounds of different bond orders are plotted versus the $^3/_2$-power of their N–N bond lengths.[34] The correlation is highlighted by a linear least-squares fit (R = 0.93) and is interesting in view of the relative positions of complexes **1** and

(31) All the samples tested are extremely sensitive to the presence of oxygen and decompose rapidly upon exposure to air.

(32) Loehr, T. M.; Sanders-Loehr, J. *Methods Enzymol.* **1993**, *226*, 431–470.

(33) Rasetti, F. *Proc. Natl. Acad. Sci. U.S.A.* **1929**, *15*, 234–237.

(34) Given that the frequency $\nu = (1/2\pi)(k/\mu)^{1/2}$, where k is the force constant and μ is the reduced mass, and the Badger's rule relationship[35] $r_e \propto k^{-1/3}$, where r_e is the equilibrium bond length, the frequency would then be proportional to $r^{3/2}$.

(35) Herschbach, D. R.; Laurie, V. W. *J. Chem. Phys.* **1961**, *35*, 458–463.

Table 1. Resonance Raman Frequencies and Proposed Assignments for the Dinuclear Zr_2N_2 Complexes **1** and **2** in the Solid and in Solution[a]

1[b] (solid)	1[c] (soln)	assgnmt	2,[d] dichloro (solid)	2,[e] dichloro (solution)	assgnmt	2,[f] dibromo	assgnmt
			132			179	
226 (+2)	225		258	262*p* (–2)	A	295	A
277			317 (–1)?	321/331*p* (–3/–4)	B		
295	289		394		C		
			448				
325	320 (–2)		515		2A		
			578	585	A + B	589	2A
			633		2B		
			710		B + C		
763			731 (–22)	733/745*p* (–23/–26)	D; ν(N–N)	710	B; ν(N–N)
			892		A + 2B		
997			991 (–23)	1002	A + D	880	3A
1012			1046 (–23)		B + D	1009	A + B
1126	1125 (–1)		1124 (–21)	1074	C + D	1167	4A
1211 (–40)	1202 (–37)	ν(N–N)	~1200			1293	2A + B
			1245 (–23)		2A + D		
			1306 (–22)		A + B + D		
			1361 (–22)		2B + D		
			1457 (–45)		2D		

[a] Frequencies in cm^{-1}; observed ^{15}N isotope shifts in parentheses. [b] $\{[(Pr^i_2PCH_2SiMe_2)_2N]Zr(\eta^5\text{-}C_5H_5)\}_2(\mu\text{-}\eta^1\text{:}\eta^1\text{-}N_2)$ (complex **1**). [c] **1** in toluene solution. [d] $\{[(Pr^i_2PCH_2SiMe_2)_2N]ZrCl\}_2(\mu\text{-}\eta^2\text{:}\eta^2\text{-}N_2)$ (complex **2**). [e] **2** in THF solution. [f] $\{[(Pr^i_2PCH_2SiMe_2)_2N]ZrBr\}_2(\mu\text{-}\eta^2\text{:}\eta^2\text{-}^{15}N_2)$; natural abundance ^{14}N data for the dibromo complex of **2** not shown.

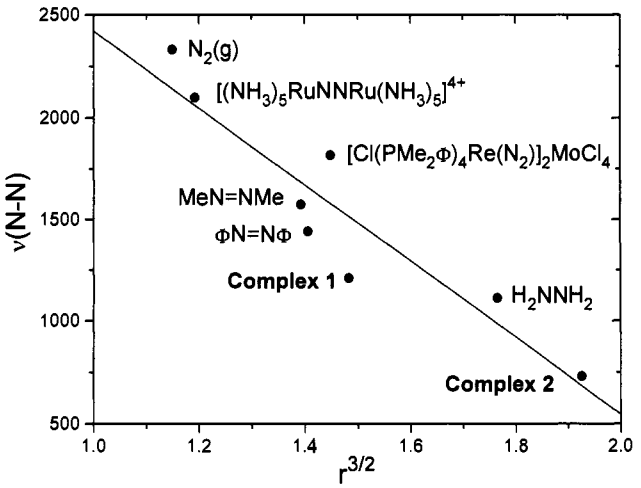

Figure 4. N–N stretching frequencies of selected dinitrogen compounds of different bond orders as a power function of their N–N bond lengths.[34]

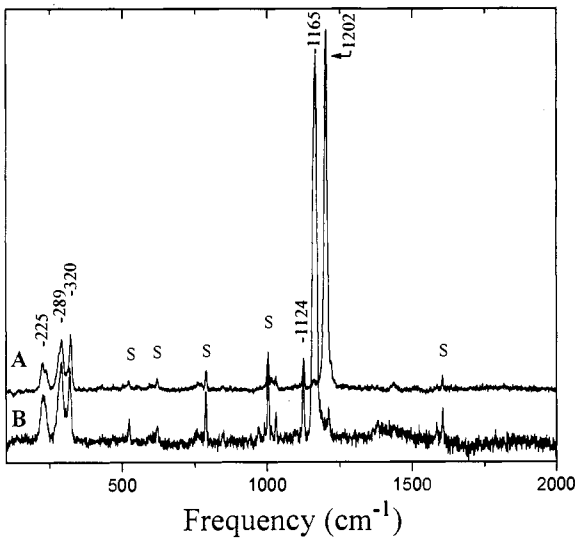

Figure 5. Resonance Raman spectra of complex **1** in toluene solution at ~90 K: (A) μ-η^1:η^1-N_2, (B) μ-η^1:η^1-$^{15}N_2$ isotopomer. Conditions were the same as in Figure 3.

2. The former lies approximately midway, in both frequency and bond length, between representative N–N single and double bond values. The point for complex **2** is quite remarkable and shows the excellent correlation between its very long bond length and its low ν(N–N) (see discussion in the following section).

The RR spectrum of complex **1** in toluene solution is nearly identical to that in the solid state (Figure 5A). The intense peak found in the solid at 1211 cm^{-1} now appears at 1202 cm^{-1}, and it shifts to 1165 cm^{-1} in the $^{15}N_2$ isotopomer (Figure 5B). This isotope shift is within 4 cm^{-1} of that predicted for a pure ν(N–N) vibrational mode. The presence of solvent also causes some spectral changes in the low-frequency region (Table 1). Nearly all other minor peaks in the spectra of **1** in solution are assignable as toluene bands,[36] as indicated in Figure 5. In both the solid and solution samples of **1**, the ~1200-cm^{-1} feature is the only band in the RR spectrum with a large ^{15}N-isotope shift. Given that the overall spectral pattern remains the same, these data strongly suggest that complex **1** in solution retains the μ-η^1:η^1-N_2 structure of the crystalline solid.

Vibrational Spectra of $Zr_2(\mu\text{-}\eta^2\text{:}\eta^2)N_2$ Complexes. The RR spectra of both isotopomers of complex **2** in the solid state and in THF solution are shown in Figures 6 and 7, respectively. Complex **2** has very different RR spectra from those of complex **1**, revealing many isotope-sensitive features, unlike the spectra of complex **1**, where only the ~1210-cm^{-1} band shifts with ^{15}N substitution. The RR spectra of complex **2** are dominated by many overtone and combination bands of only a few fundamentals. These spectral properties are undoubtedly related to the side-on coordination of the N_2 ligand, examples of which are still rare.[17]

The two most intense peaks found in the solid-state spectra of complex **2** are found at 317 and 731 cm^{-1} (Figure 6A). In addition, many peaks of lower intensity are observed between 100 and 1500 cm^{-1}. Frequencies and proposed assignments are given in Table 1. The peaks at 731, 991, and 1045 cm^{-1} shift to 709, 968, and 1023 cm^{-1}, respectively, upon $^{15}N_2$ substitution (Figure 6B). The 22-cm^{-1} isotope shift observed for the 731-cm^{-1} peak is within 3 cm^{-1} of that expected for a pure ν(N–N) mode at this frequency, suggesting that this feature is one of the totally symmetric A_g modes of the Zr_2N_2 moiety. One may compare this value with ν(N–N) of liquid hydrazine at 1111 cm^{-1}.[37] If vibrational frequencies are used to estimate the bond order (and the N–N

(36) Strommen, D. P.; Nakamoto, K. *Laboratory Raman Spectroscopy*; Wiley: New York, 1984.

(37) Durig, J. G.; Bush, S. F.; Mercer, E. E. *J. Chem. Phys.* **1966**, *44*, 4238–4247.

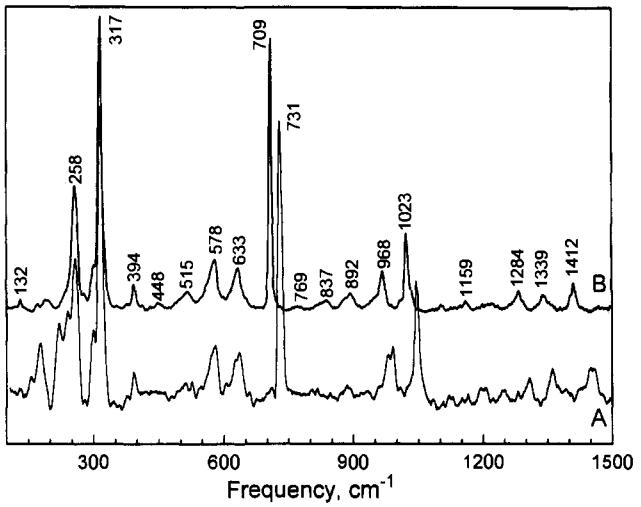

Figure 6. Resonance Raman spectra of complex **2** in the solid state at ~90 K: (A) μ-η^2:η^2-N_2, (B) μ-η^2:η^2-$^{15}N_2$ isotopomer. Each trace is a sum of 9 consecutive scans each recorded at 1 cm^{-1}/s using 20 mW of 647.1-nm laser excitation. [The group of three bands at ~170, 220, and 240 cm^{-1} (trace A) appeared with variable intensities in repeat experiments, although no changes were noted in the remaining spectral peaks; these features are, therefore, attributed to decomposition products.]

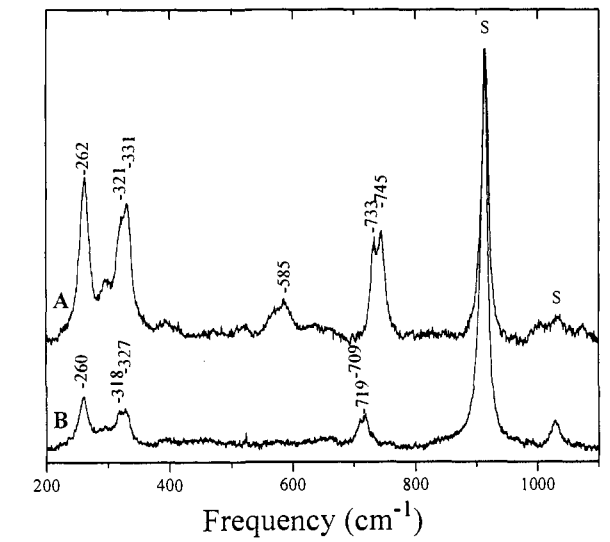

Figure 7. Resonance Raman spectra of complex **2** in THF solution at ~90 K: (A) μ-η^2:η^2-N_2, (B) μ-η^2:η^2-$^{15}N_2$ isotopomer. Each trace is a sum of 5 consecutive scans each recorded at 1 cm^{-1}/s using 40 mW of 647.1-nm laser excitation.

bond length, as in Figure 4), and, further, if the 731-cm^{-1} peak represents the principal ν(N–N) stretching mode, then the N–N bond order of complex **2** is *significantly lower* than that in hydrazine, which is assumed to have an N–N bond order of 1. This surprisingly low bond order is consistent with the very long and unique N–N bond of 1.548 Å observed in the crystal structure.[21,29]

The other isotope-sensitive peaks of **2** (Figure 6 and Table 1) are assigned as follows: The 991-cm^{-1} peak, which has an isotope shift of 23 cm^{-1} in the $^{15}N_2$-enriched sample, is a combination of the 258- and 731-cm^{-1} bands. This assignment is supported by the fact that the 731-cm^{-1} band shifts 22 cm^{-1} in the $^{15}N_2$-enriched sample but the 258-cm^{-1} band is isotope insensitive. Similarly, the peak at 1046 cm^{-1} is assigned as the combination of the 317- and 731-cm^{-1} peaks based on its observed 23-cm^{-1} shift. In addition, two other isotope-sensitive bands at 1306 and 1361 cm^{-1} that shift by –22 cm^{-1} to 1284 and 1339 cm^{-1}, respectively, are assigned as further combinations of the frequencies at 317 + 991 cm^{-1} and 317 + 1046 cm^{-1}, respectively. The band at 1457 cm^{-1} is assigned as the first overtone of the 731-cm^{-1} ν(N–N) mode. This identification is supported by its large (~45 cm^{-1}) isotope shift that is twice that observed for the 731-cm^{-1} fundamental. Many of the remaining peaks are also simple combination and overtone bands. For instance, the 579-cm^{-1} band is a combination of the 258- and 317-cm^{-1} modes and the 633-cm^{-1} band is the first overtone of the 317-cm^{-1} signal. Also, the 515-cm^{-1} peak is assigned as the first overtone of the 258-cm^{-1} band based on its isotope insensitivity. A nearly complete set of assignments for the frequencies of the solid of complex **2** in the 150–1500-cm^{-1} range that is consistent with the observed isotope shifts is given in Table 1.

Complex 2 in Solution. At first glance, the RR spectra of complex **2** in solution appear quite different from those in the solid state; however, these dilute solution spectra are dominated by the strong THF band at ~914 cm^{-1}.[36] The 731-cm^{-1} peak of complex **2** in the solid is split into a pair of signals at 745 and 733 cm^{-1} in THF solution (Figure 7A). These shift to 719 and 709 cm^{-1}, respectively, in the $^{15}N_2$ isotopomer (Figure 7B). Both isotope shifts are within 1 cm^{-1} of the predicted value for a pure ν(N–N) vibrational mode at this frequency and are identical in magnitude to that observed for the 731-cm^{-1} peak of complex **2** in the solid state. Similarly, the 317-cm^{-1} feature in the spectrum of the solid of **2** is also split into a pair of peaks at 331 and 321 cm^{-1}, respectively, in the RR spectrum of the solution sample. These are seen to shift –4 to –3 cm^{-1}, respectively, in the ^{15}N isotopomer, unlike the relatively insensitive low-frequency bands of the solid sample. Two poorly resolved, weak peaks are also apparent at 1002 and 1074 cm^{-1} (Figure 7A). The intense peak at 262 cm^{-1} in the solution sample shifts –2 cm^{-1} in the isotopomer; however, the apparent combination band of weak-to-medium intensity at ~585 cm^{-1} is absent in the spectrum of the $^{15}N_2$ isotopomer, and may be attributed to the low concentration in the isotopically enriched sample.

Polarization studies of the $^{15}N_2$ isotopomer in solution show that the 719/709-cm^{-1} pair is polarized (ρ = 0.32), further supporting the suggestion that this is one of the totally symmetric A_g modes. The 260-cm^{-1} peak and the 318/327-cm^{-1} pair also appear to be polarized (ρ = 0.35 and 0.40, respectively). The lower depolarization ratio of the 260-cm^{-1} peak suggests that this may be the second A_g mode of the Zr_2N_2 cluster; however, we cannot rule out the possibility that the 318/327-cm^{-1} pair may also share some A_g character. Even without complete assignments of these bands at this time, the two strong peaks in the low-frequency region, together with a strong isotope-sensitive peak in the ~735-cm^{-1} region, are very similar to corresponding peaks in the solid-state spectrum (Figure 6), indicating that the side-on geometry of the bridging N_2 ligand is preserved in THF solution.

Vibrational Spectra of $Zr_2(\mu$-η^2:η^2-$^{15}N_2)$ Complexes with Mixed Halogen Ligands. The crystal structure of complex **2** indicates that the molecule possesses a center of symmetry.[21] For centrosymmetric molecules, only vibrational modes of *g* symmetry are spectroscopically allowed in the Raman effect.[38] Therefore, RR experiments were conducted on samples of complex **2** containing both Cl^- and Br^- ligands to determine if the loss of the center of symmetry would cause any new fundamental modes to appear in the spectra.

The resonance Raman spectra of the dichloro complex, $\{[(Pr^i_2PCH_2SiMe_2)_2N]ZrCl\}_2(\mu$-$\eta^2$:$\eta^2$-$^{15}N_2)$, the mixed bromochloro complex, $\{[(Pr^i_2PCH_2SiMe_2)_2N]Zr\}_2ClBr(\mu$-$\eta^2$:$\eta^2$-$^{15}N_2)$, and the dibromo complex, $\{[(Pr^i_2PCH_2SiMe_2)_2N]ZrBr\}_2(\mu$-$\eta^2$:$\eta^2$-$^{15}N_2)$, are shown in Figure 8. NMR spectra of the bromochloro sample indicate that it is a 1:2:1 mixture of the dichloro, the bromochloro, and the dibromo species, respectively. Comparison of the RR spectra of the three halogenated forms of complex **2** shows that the peaks at 258 and 317 cm^{-1} (Figure 8A) begin to merge in the

(38) Harris, D. C.; Bertolucci, M. D. *Symmetry and Spectroscopy*; Oxford: New York, 1978.

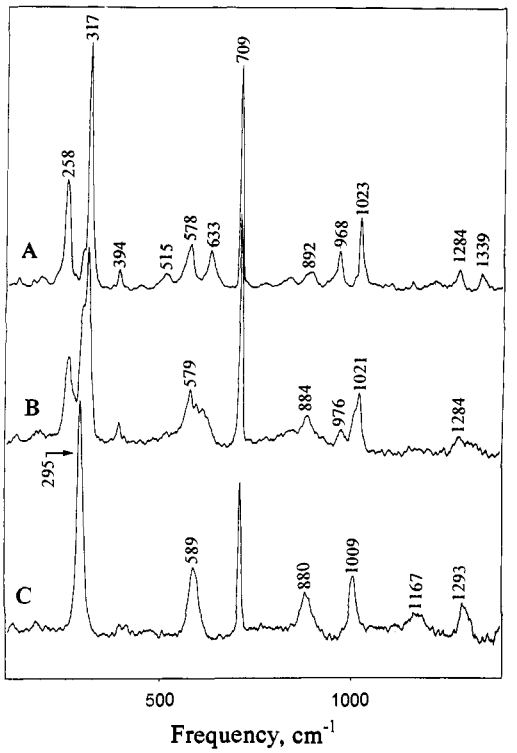

Figure 8. Resonance Raman spectra of derivatives of complex **2** with different halogen ligands in the solid state at ~90 K; in each case, only the spectra of the $^{15}N_2$ isotopomers are shown: (A) the parent compound, $\{[(Pr^i_2PCH_2SiMe_2)_2N]ZrCl\}_2(\mu\text{-}\eta^2\text{:}\eta^2\text{-}^{15}N_2)$, as in Figure 6B; (B) $\{[(Pr^i_2PCH_2SiMe_2)_2N]Zr\}_2BrCl(\mu\text{-}\eta^2\text{:}\eta^2\text{-}^{15}N_2)$, a 1:2:1 mixture of the dichloro, the bromochloro, and the dibromo complexes, respectively; and (C) $\{[(Pr^i_2PCH_2SiMe_2)_2N]ZrBr\}_2(\mu\text{-}\eta^2\text{:}\eta^2\text{-}^{15}N_2)$. Spectral conditions were the same as in Figure 6.

mixed halogenated sample (Figure 8B), and in the fully brominated sample, only a single peak remains at 295 cm^{-1} (Figure 8C). We had expected that replacement of Cl^- by Br^- would cause a new peak to develop at <200 cm^{-1} corresponding to ν(Zr–Br); however, no new peaks could be observed between 50 and 200 cm^{-1} in the RR spectrum of the dibromo complex of **2** (data not shown). Similarly, the 515-, 578-, and 633-cm^{-1} peaks in Figure 8A converged to a single peak at 589 cm^{-1} in Figure 8C. In addition, new peaks were found at 880, 1009, 1167, and 1293 cm^{-1} (Figure 8C).

Clearly, the peaks observed at 589, 880, and 1167 cm^{-1} for the dibromo complex (Figure 8C) represent the first, second, and third overtone, respectively, of the fundamental mode at 295 cm^{-1}. Furthermore, the 1293-cm^{-1} peak is a combination band representing the sum of the fundamental mode at 709 cm^{-1} and the first overtone band at 589 cm^{-1}. The 1009-cm^{-1} peak is assigned as the combination of fundamentals at 710 and 295 cm^{-1}.

In short, replacement of the Cl^- ligand with Br^- causes some of the overtone and combination bands to disappear in the low- and medium-frequency region while inducing new overtones in the high-frequency region. Nevertheless, no new fundamental modes of the Zr_2N_2 moiety become visible upon replacement of Cl^- ligands for Br^- or by reduction of symmetry. Moreover, ignoring the combination and overtone bands, the overall spectral pattern is quite similar among spectra A, B, and C in Figure 8, suggesting that the side-on geometry of the N_2 ligand is preserved in each case.

Conclusions

This work has shown that resonance Raman spectroscopy can be used to clearly identify and distinguish the two modes of bonding for a dinitrogen ligand in dinuclear metal complexes in both the solid and solution states. Zirconium compounds with a bridging N_2 ligand give radically different RR spectra depending on the geometry of N_2 binding. For complex **1**, a single intense peak is found in the RR spectrum at 1211 cm^{-1} corresponding to the ν(N–N) symmetric stretch that shifts to 1172 cm^{-1} in the $^{15}N_2$-enriched isotopomer. This value corresponds to an N–N bond order between 1 and 2, consistent with the 1.301-Å N–N bond length observed in the crystal structure. Comparison of solution and solid state spectra shows excellent correlation of features, indicating that the structures of complex **1** as a solid and in toluene solution are nearly identical.

For complex **2**, there is more than one isotope-sensitive feature in the RR spectra, complicating the assignment. Nevertheless, there is strong evidence to support the conclusion that the 731-cm^{-1} peak is a totally symmetric mode composed primarily of ν(N–N) character. The other isotope-sensitive bands are assigned as the combination of the peaks found at 731, 317, and 258 cm^{-1}. The vibrational assignment of complex **2** in THF solution is further complicated by the splitting of peaks. Nevertheless, the presence of isotope-sensitive features below 1111 cm^{-1} implies an N–N bond order of less than 1, a deduction supported by the 1.548-Å N–N bond length observed in the crystal structure. More importantly, the positions of the fundamental modes in the solution state spectra are quite similar to those of the fundamentals in the solid state, providing further evidence that the overall geometry of the Zr_2N_2 moiety is preserved when complex **2** is in solution.

Finally, the effect of replacing Cl^- with Br^- as ligands is to alter the number of observed combination and overtone bands in the RR spectrum. However, neither replacing one halogen ligand with another halogen nor eliminating the center of symmetry was sufficient to cause any new normal modes to appear in the RR spectra.

The exact site of nitrogen coordination in nitrogenase and the mechanism of the subsequent reduction are still open questions.[7] The unique molybdenum atom of the FeMo cofactor, long suspected to be important in nitrogen binding and activation, appears to be coordinatively saturated, being bound to three sulfur atoms and a histidyl nitrogen and chelated to two oxygen atoms of homocitrate.[5,6] A recent selenium-EXAFS study shows that selenols are competent to bind to iron, but not molybdenum.[39] Thus, it is possible that iron atoms provide the site of initial coordination and reduction of N_2.[40] The Zr_2N_2 compounds of the present study show that N_2 bridging between metals may be accompanied by extreme elongation of the N–N bond. In the case of the $\mu\text{-}\eta^2\text{:}\eta^2$ structure, the resulting N–N bond is considerably longer than that in hydrazine.

Acknowledgment. This work was supported by grants from NSERC to M.D.F. and the National Institutes of Health (GM34468 to T.M.L.). Purchase of instrumentation in the Raman spectroscopy laboratory at OGI was made possible, in part, by a Shared Instrumentation Grant from the National Institutes of Health (S10 RR02676). We thank Dr. Jie Sun for helpful comments and insights.

(39) Conradson, S. D.; Burgess, B. K.; Newton, W. E.; Di Cicco, A.; Filipponi, A.; Wu, Z. Y.; Natoli, C. R.; Hedman, B.; Hodgson, K. O. *Proc. Natl. Acad. Sci. U.S.A.* **1994**, *91*, 1290–1293.

(40) Leigh, G. J.; Jimenez-Tenorio, M. *J. Am. Chem. Soc.* **1991**, *113*, 5862–5863.